International Journal of Heat and Mass Transfer 52 (2009) 1725–1733

Contents lists available at ScienceDirect

International Journal of Heat and Mass Transfer

journal homepage: www.elsevier.com/locate/ijhmt

Thermodiffusion in porous media: Multi-domain constitutant separation

R. Bennacer [a], A.A. Mohamad [b,*], M. El Ganaoui [c]

[a] LEEVAM, IUT-GC-Cergy-Pontoise Univ., Neuville sur Oise, 95031, France
[b] Dept. of Mech. Eng., Schulich School of Eng., Univ. of Calgary, AB, Canada T2N 1N4
[c] Univ. of Limoges, CNRS/SPCTS, Fac. Sci. et Tech, 123 Av. Albert Thomas, 87060 Limoges, France

ARTICLE INFO

Article history:
Received 27 September 2007
Received in revised form 11 September 2008
Available online 4 December 2008

ABSTRACT

A numerical study is carried out on double-diffusive, natural convection within a vertical annular, porous cylinder. The flow is driven by buoyancy force due to externally applied constant temperature difference on the vertical cylinder while the horizontal surfaces are impermeable and adiabatic. The effects of cross phenomena "Soret effect" were considered in the analysis. It is demonstrated that the cylindrical annulus permits a higher thermal gradient. It is established that such system has an optimal separation effect for a given thermal Rayleigh number, Ra_T. To overcome such limitation, two sub-domains (buffer) allowing filtration separation was proposed and investigated. The flow field, temperature and concentration distributions are obtained in terms of the governing parameters. The effect of the sub-domains scales, the Darcy number, *Da*, and the curvature, *R*, on flow, temperature and species separation ability is found to be significant.

1. Introduction

Double-diffusive, natural convection in porous media has been extensively investigated in recent years, owing to relevance in various applications. Interest in this phenomenon has been motivated by diverse engineering problems such as the drying processes, migration of moisture contained in fibrous insulation, grain storage installations, food processing, chemical transport in packed-bed reactors, contamination transport in saturated soil, the underground disposal of nuclear wastes, etc.

Authors focused on the in enclosures (cavities or confined media between vertical cylinder) to study numericaly the natural convection on porous media or under parallel flows [1–3]. However, most of the research efforts have been devoted to the flow caused by a single buoyancy effect, namely the temperature gradient. The numerical works of Havstad and Burns [4], Reda [5] Prasad and co-workers [6–7] and Hasnaoui et al. [8] resulted on various correlations for the heat transfer rates. Recently, Bennacer et al. [9–10] investigated the effects of the thermal Rayleigh and Lewis numbers on flow structures and average Nusselt and Sherwood numbers for a closed vertical cylindrical annulus filled with a binary liquid.

Early investigations on the role of the Soret effect in natural convection of binary fluids primarily focused on the problem of convective instability in a horizontal layer. A review of such studies is given by Platten and Legros [11] including the ternary systems. In the last decade, this problem has gained a renewed interest both theoretical and experimental (for instance see Refs. [11–12]). More recently, Larre et al. [13] investigated the stability of a triple diffusive fluid layers heated from below. By incorporating the cross diffusion effects with stability analysis of the stable (base) state, the resulting critical parameters for the onset of convection were found to be in agreement with experiments.

The influence of the Soret effect on the flow structure in a square cavity, where a binary fluid is subjected to thermal and concentration gradients, has been investigated by Traore and Mojtabi [14] and for a thermal gradient in a tall cavity by Labrosse [15]. The existence of two regimes for the concentrations fields, namely a pure diffusive regime and boundary layer regime, has been discussed by those authors. Based on the numerical work of Havstad and Burns [4], Reda [5] Prasad and co-workers [6,7] and Hasnaoui et al. [8], various relative useful correlations for heat transfer rates have been reported by the authors, as mentioned before. Bennacer et al. [16] and Lakhal et al. [17] have investigated the effects of varying the thermal Rayleigh and Lewis numbers on flow structures and average Nusselt and Sherwood numbers for a closed vertical cylindrical annulus filled with a binary liquid.

The present study analyzes the cross phenomena "Soret effect" in an annular cylinder filled with porous medium. The main focused on work is on the effect of curvature on the separation ability of such a system. A new technique for a higher separation performance is demonstrated.

* Corresponding author. Tel.: +1 403 220 2781; fax: +1 403 282 8406.
E-mail addresses: rachid.bennacer@u-cergy.fr (R. Bennacer), mohamad@ucalgary. ca (A.A. Mohamad).

0017-9310/$ - see front matter © 2008 Elsevier Ltd. All rights reserved.
doi:10.1016/j.ijheatmasstransfer.2008.09.026

Nomenclature

A	annulus aspect ratio, A = e'/H'
C'	concentration,
D	molecular diffusion
D_S	thermodiffusion coefficient
Da	Darcy number, K/e'^2
e'	width of porous annulus, $r'_e - r'_i$, m
H'	height of the enclosure, m
k	radius ratio (curvature), $k = r_e/r_i$
K	permeability of the porous medium, m^2
N	buoyancy ratio, $N = \beta_C \Delta C'/\beta_T \Delta T'$
r	dimensionless radial space co-ordinate, r'/e
R	curvature, e/r'_i
R_D	molecular diffusion ratio (effective to fluid)
R_λ	thermal conductivity ratio (effective to fluid)
Ra_C	solutal Grashof number, β_C g $\Delta C'$ $e'^3/(\upsilon D)$
Ra_T	thermal Grashof number, β_T g $\Delta T'$ $e'^3/(\upsilon\alpha)$
T	dimensionless temperature, $(T' - T'_0)/\Delta T'$
Z	dimensionless vertical space co-ordinate,

Greek symbols

α	effective thermal diffusivity, m^2/s
β	coefficient of expansion,
$\Delta C'$	concentration difference between vertical boundaries,
ΔT	temperature difference between vertical boundaries,
ε	porosity
Λ	apparent viscosity
υ	kinematics viscosity, m^2/s^{-1}
ρ	fluid density, kg m^{-3}
σ	heat capacity ratio, $(\rho C)_p/(\rho C)_f$
ψ	dimensionless stream function, ψ'/ν

Superscript

'	dimensional variable

Subscript

C	cold
eff	effective (equivalent)
f	fluid
H	hot
I	inner cylinder
L	liquid
0	outer cylinder
P	porous

2. Model

Consider a fluid-saturated, porous layer enclosed between two concentric cylinders as shown in Fig. 1-a, the height of the layer is denoted by H and the inner and outer radius by r'_i and r'_o, respectively. All boundaries of the annular region are impermeable. Both horizontal boundaries of the enclosure are thermally insulated while the inner and outer vertical boundaries are kept at a uniform but different constant temperature. Gravity acts in the z - direction. The porous matrix is assumed to be rigid and in thermal equilibrium with the fluid, and thermophysical properties of the solid and fluid are assumed to be constants, except density in buoyancy term. The flow is assumed to be laminar and incompressible and the Boussinesq approximation is assumed to be valid. The cross contribution "Soret effect" is taken into account where the mass flux is given by:

$$j' = -\rho(D\nabla C' + D_S C'_0(1 - C'_0)\nabla T') \tag{1}$$

where D is the mass diffusivity and D_S the phenomenological coefficients for the Soret coefficients.The following dimensionless variables (primed quantities are dimensional) are used:

$$(r,z) = (r',z')/e, \qquad (u,w) = (u',w')e/\upsilon$$
$$t = t'\upsilon/e^2, p = p'(\rho_0 \upsilon^2/e^2)$$
$$\Delta T' = T_H - T_C, \Delta C = -D_S/DC_0(1 - C_0)\Delta T'$$

where u' and w' are the volume averaged velocity components, p' is the hydrodynamic pressure, t' is the time, α, k and v are the thermal diffusivity, thermal conductivity, and kinematic viscosity of the fluid mixture, respectively. $\Delta T'$ is a characteristic temperature difference and $\Delta C'$ is the corresponding value for the constituent. The density, ρ, of the mixture is related to the temperature and solute concentration by a linear equation of state:

$$\rho(T', C') = \rho_o[1 - \beta_T(T' - T'_o) - \beta_C(C' - C'_0)] \tag{2}$$

where β_T and β_C are the thermal and solutal expansion coefficients, respectively, and subscript o indicates a reference state.The dimensionless conservation equations of mass, momentum, energy and species are

$$\frac{\partial(ru)}{r\partial r} + \frac{\partial w}{\partial z} = 0 \tag{3}$$

$$\frac{1}{\varepsilon}\frac{\partial u}{\partial t} + \frac{1}{\varepsilon^2}\left(u\frac{\partial u}{\partial r} + w\frac{\partial u}{\partial z}\right) = -\frac{\partial P}{\partial r} - \frac{u}{Da} + \Lambda\left[\nabla^2 u - \frac{u}{r^2}\right] \tag{4}$$

$$\frac{1}{\varepsilon}\frac{\partial w}{\partial t} + \frac{1}{\varepsilon^2}\left(u\frac{\partial w}{\partial r} + w\frac{\partial w}{\partial z}\right) = -\frac{\partial P}{\partial z} - \frac{w}{Da} + \Lambda\nabla^2 w + Pr^{-1}Ra_T(T + NC) \tag{5}$$

$$\sigma\frac{\partial T}{\partial t} + u\frac{\partial T}{\partial r} + w\frac{\partial T}{\partial z} = Pr^{-1}\nabla(R_\lambda \nabla T) \tag{6}$$

$$\varepsilon\frac{\partial C}{\partial t} + u\frac{\partial C}{\partial r} + w\frac{\partial C}{\partial z} = Sc^{-1}(R_D\nabla^2 C - \nabla^2 T) \tag{7}$$

The above equations identify that the problem is governed by different dimensionless parameters, namely: thermal Rayleigh number, $Ra_T = g\beta_T \Delta T' e'^3/(\upsilon\alpha)$, Prandtl number, $Pr = \upsilon/\alpha$, Schmidt number, $Sc = \upsilon/D$, buoyancy ratio, $N = \frac{\beta_C}{\beta_T}\frac{D_S}{D}C'_0(1 - C'_0)$. The parameters that characterise the flow in porous media are the Darcy number $Da = K/e'^2$, the relative thermophysics properties $\Lambda = \mu_{eff}/\mu_f$, $R_\lambda = \lambda_{eff}/\lambda_f$, $R_D = D_{eff}/D_f$ and the porosity ε. The geometry is characterised by the annulus aspect ratio $A = e'/H$, curvature $k = r_e/r_i$ (or $R = e'/r'_i = k - 1$) where e is the width of the considered domain.

The dimensionless boundary conditions on the vertical walls and horizontal surfaces are as follow:

$$\begin{aligned} &r = 1/R \quad T = 0.5 \quad \frac{\partial C}{\partial r} = \frac{\partial T}{\partial r} \\ &R = \frac{R+1}{R} \quad T = 0.5 \quad \frac{\partial C}{\partial r} = \frac{\partial T}{\partial r} \\ &Z = 0, 1/A \quad \frac{\partial T}{\partial z} = 0 \quad \frac{\partial C}{\partial z} = 0 \end{aligned} \tag{8}$$

The mentioned governing Eqs. (3)–(7) subject to boundary conditions (8) are solved by adapting a finite volume approach [18]. Convective and diffusive fluxes are respectively approximated using a second order central scheme. For more details about the numerical method, we refer to [19].

The accuracy of the numerical method has been established with reference solutions concerning pure thermal and thermosolutale convection within a rectangular anisotropic porous cavity [20]. Grid size dependency is studied by verifying the variation of the predicted results from coarse one 81×81 to refined one

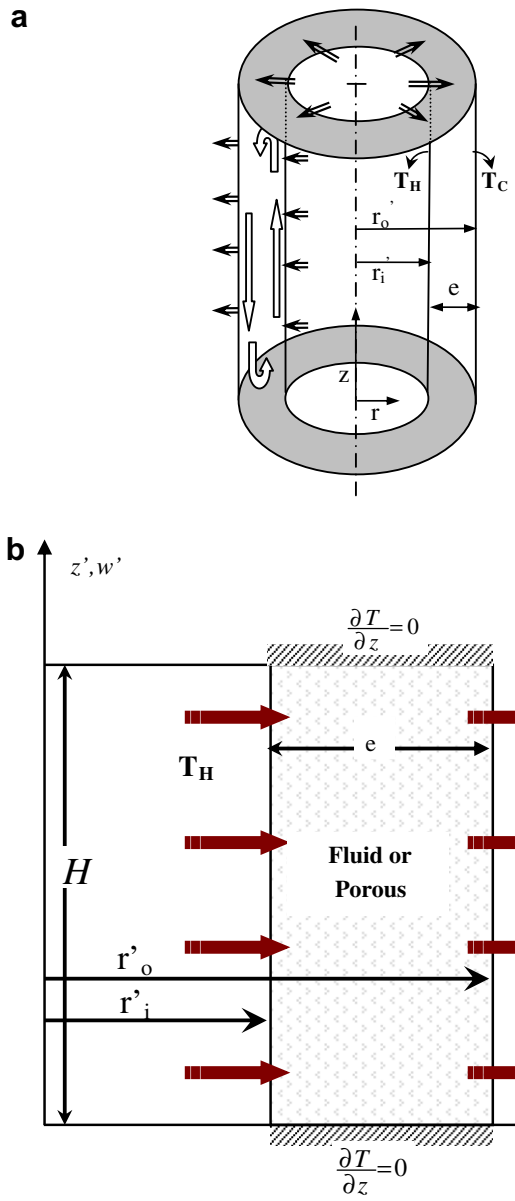

Fig. 1. Configuration of the problem (physical model) (a) and domain of integration (b).

251×251(non-uniform). The grid numbers of 131×131 (non-uniform) give a good compromise between accuracy and CPU time are used in producing the results.

3. Results

It needs quite extensive analysis to cover effects of each parameter. It is intended to limit the analysis for Prandtl number of 10, and $Le = 10$ and for an aspect ratio of 1/2. Also, the value 1 was used for ε, R_{λ}, R_D and Λ in all the calculations.

3.1. Diffusive regime

For low Rayleigh number ($Ra_T \sim 0$) the obtained solution is diffusive. In such regime, the radial temperature profile is logarithmic, which depends on the curvature. For low curvature ($R \sim 0$), the temperature profile is almost linear (Cartesian domain). The effect of inner radius on the obtained steady state temperature profile is represented in Fig. 2. The figure illustrates clearly the

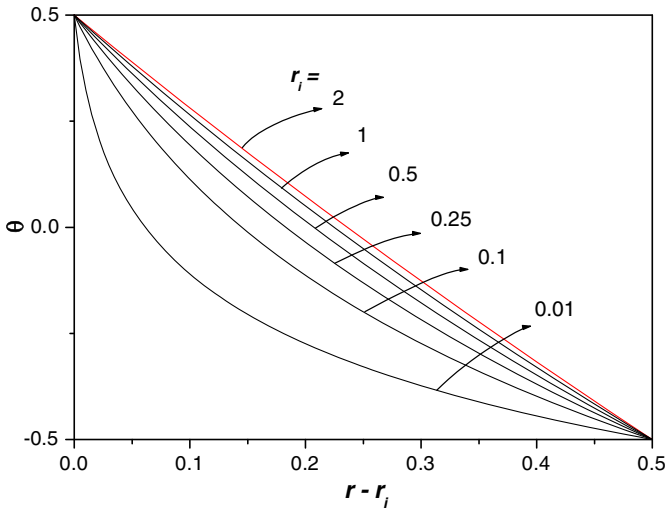

Fig. 2. The effect of curvature on the obtained purely diffusive temperature profile.

increase (decrease) of the temperature gradient near the inner (outer) cylinder surface. The specie separation under Soret effect depends on the temperature gradient and such change in temperature gradient will affect the obtained solutal field. It is obvious that the solutal gradient will be the same as temperature gradient (see boundary condition, Eq. (8)).

The effect of inner radius on the obtained steady state concentration profile is represented in Fig. 3. The solutal gradient increases (decreases) near the inner (outer) surface of the cylinder.

In diffusive regime the temperature profile resulting, under fixed temperature or flux boundary condition, is included in the set [−0.5 to 0.5]. This is due to the imposed temperature values on the borders of the considered domain. In convective regime, the solutal and temperature field are different, despite the same applied gradients (Eq. (8)) on the inner and outer cylinder. Such difference is a consequence of:

the temperature-concentration diffusion difference ($Le \neq 1$)
the global species conservation due to closed system as explained in next section.

In the initial condition, the binary fluid is at homogeneous concentration, C_0, the applied temperature difference induce a separation. So, an increase of the concentration in the vicinity of the inner cylinder is obtained ($\Delta C_1 = C_{max} - C_0$) and corresponding decrease in the vicinity of the outer cylinder ($\Delta C_2 = C_0 - C_{min}$) should be noticed. The species separation must satisfy the conservation equality between the obtained steady state profile and the initial homogeneous concentration C_o:

$$\int_{r_o}^{r_i} C'(r) r' dr' = C'_0\left(r_0'^2 - r_i'^2\right)/2 = \text{constant}$$

The obtained concentration profile has to satisfy the boundary condition (Eq. (8)) the model (Eq. (7)) and the constant overall concentration in the domain. In Cartesian domain (centrosymetry problem) we obtain $\Delta C_1 = \Delta C_2$ but the in the cylindrical geometry (section function of r) the concentration increase is more important than the decrease, i.e. $\Delta C_1 > \Delta C_2$.

The maximum difference between the two cylindrical surfaces (in diffusive) is always equal to unity. This is a direct consequence of our reference concentration difference:

$$\Delta C' = -\frac{D_s}{D} C'_0 (1 - C'_0) \Delta T'$$

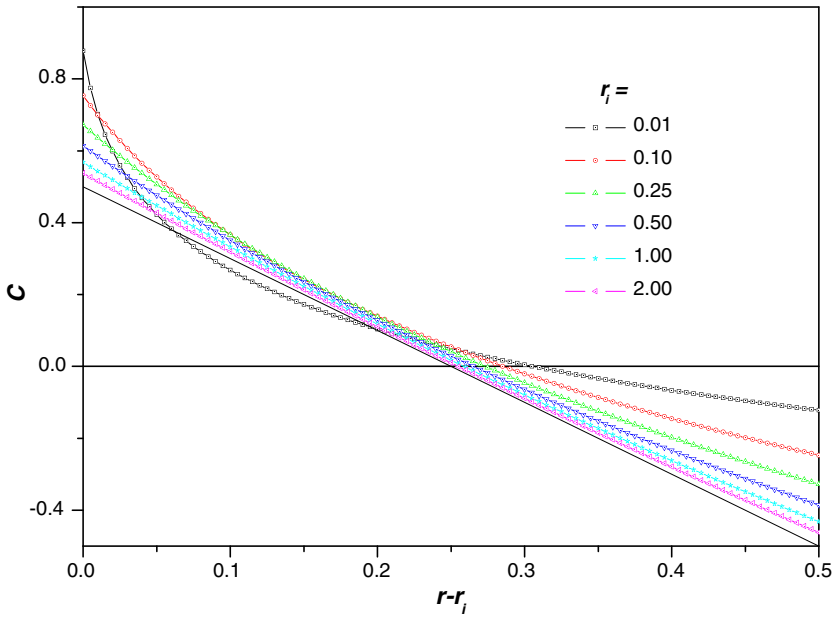

Fig. 3. The effect of curvature on the obtained purely diffusive concentration profile.

The separation improvement can be achieved by increasing the temperature difference in the solution domain. However, the increase in ΔT induces convective flow and destroys the solutal separation ability. This issue will be discussed in the next section.

The obtained limits (C_{max} and C_{min}) of the concentration on the two surfaces of the cylinder are represented in Fig. 4, for different curvature. For low curvature (r_i) corresponding to the Cartesian domain we have a linear and symmetrical field around C_0, i.e. $C_{max} = 0.5$ and $C_{min} = -0.5$. The separation ability (for chosen a species) increases with curvature and tend to the asymptotical value of unity for the high curvature values.

It is demonstrated that, in the diffusive regime, the utility of using cylindrical configuration allows doubling the separation ability compared with plane geometries.

The possible existing flow can be considered as perturbative phenomena, where the advective term affects the solutal field and enhances the mixing process. We previously underline the increase in temperature and concentration gradient with curvature and such increase induce stronger buoyancy forces resulting in natural convection.

Convective regime The fluid flow and Soret effect can be contribute to better separation ability. The Soret effect is used in the horizontal direction as solutal pump and the vertical flow allow the drag of the species A to the top and the specie B to the bottom of the domain. This allows separation and easy extraction from reduced domain in the top and the bottom.

For a very low Ra_T, the problem is diffusive and the solutal concentration between the top and the bottom is very weak as shown in Fig. 5 (for more analysis see Lakhal [21]).

For a given flow, the mixing and solutal transport of the rich specie (weak) take place at the top (bottom) of the domain.

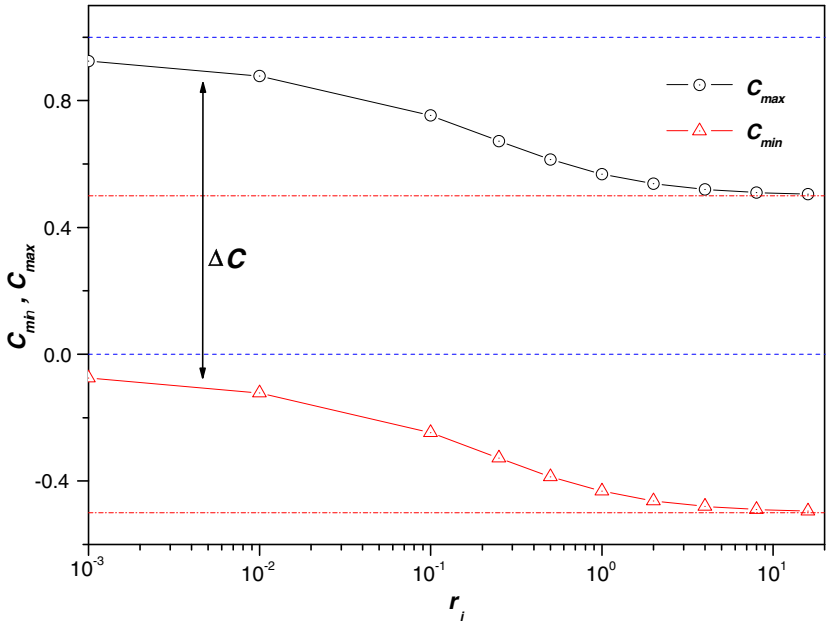

Fig. 4. The effect of curvature on the obtained maximum and minimum concentration in the domain.

For such condition, we have a vertical separation in the vertical direction. The species separation increases with Ra_T until an optimum value obtained for a given Ra_T (Fig. 5). An example of the obtained temperature, concentration and vertical velocity component on the horizontal mid plan is represented in Fig. 6. This figure clearly illustrates the flow mixing ability where we can see that the maximum concentration value on the inner cylinder is 0.2 in compared with 0.5 obtained in the diffusive regime. The figure illustrates also that the solutal boundary layer is thinner than the thermal one because the Lewis number is greater than unity.

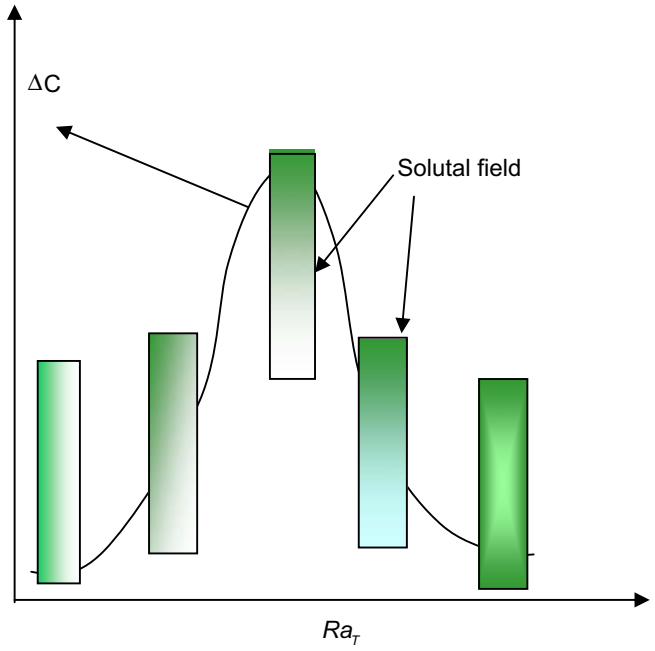

Fig. 5. The effect of the Ra_T number on the obtained vertical species separation and *Sh*.

The specie concentration is more sensitive to the flow (if Le > 1), the convective flow increases with increase in Ra_T, consequently the mixing increases and the specie separation decreases, until reaches complete mixing, where no separation takes place (Fig. 5).

The previous numerical and analytical results (boundary layer approach) showed the existence of bell shape (see Fig. 5) in separation ability versus Ra_T number in Cartesian domain. In present work also showed the bell shape distribution in the cylindrical domain.

For high Ra_T number, the flow is so strong that the convective mixing not allows for separation to be significant. To overcome such limitation a porous media can be used, as we did in our previous work [13–14]. The classical separation in fluid domain or porous domain can be improved by the cylindrical configuration but the obtained concentration values in diffusive regime remain the asymptotical limit separation.

The partitioning domain is added to enhance the filtration and separation processes. The new configuration is represented in Fig. 7. The buffer communicates with the global domain by a thin connection, through porous media (Fig. 7b), allowing extraction of low (high) concentration with weak flow. However, the size of this porous medium and his permeability affect the result. The main advantage of such system is the cross flow on the two surface of the porous media. As all the convective cells are clockwise, on the upper surface of the porous layer we have a cold flow and at the bottom of the porous layer a hot flow. The cross flow, as represented in Fig. 7b generates a strong thermal gradient. As the Soret contribution is directly related to the thermal gradient, the process of separation enhances.

In the present study and in order to illustrate such advantage, the numerical results are presented for the three mentioned configurations represented on Fig. 8:

1. Full porous domain.
2. Partitioned domain in three part using solid horizontal walls (R = sol/liq = 0.01).

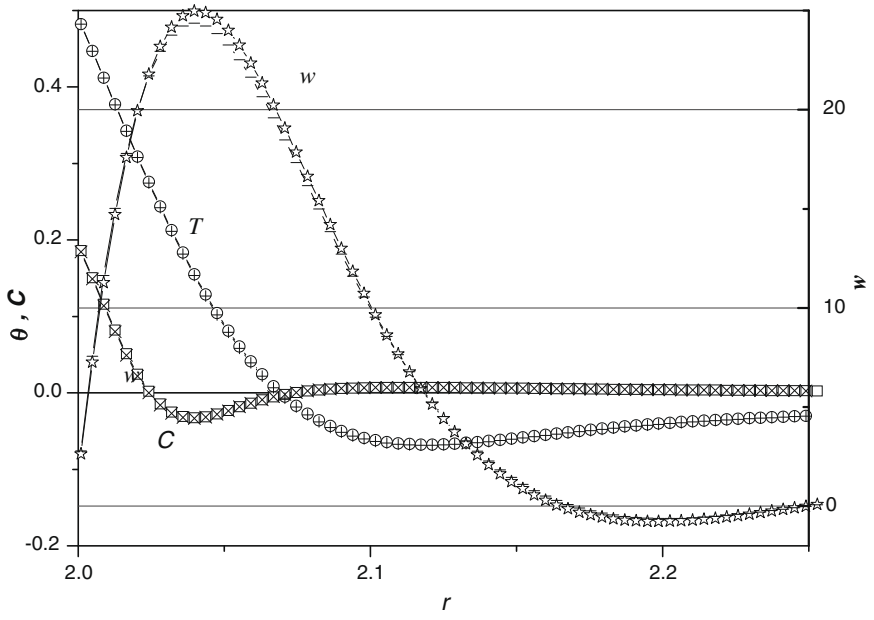

Fig. 6. Temperature, concentration and vertical velocity component on the horizontal mid-plan ($Ra_T = 10^5$, $Pr = 10$, $Le = 10$ and $N = 0$).

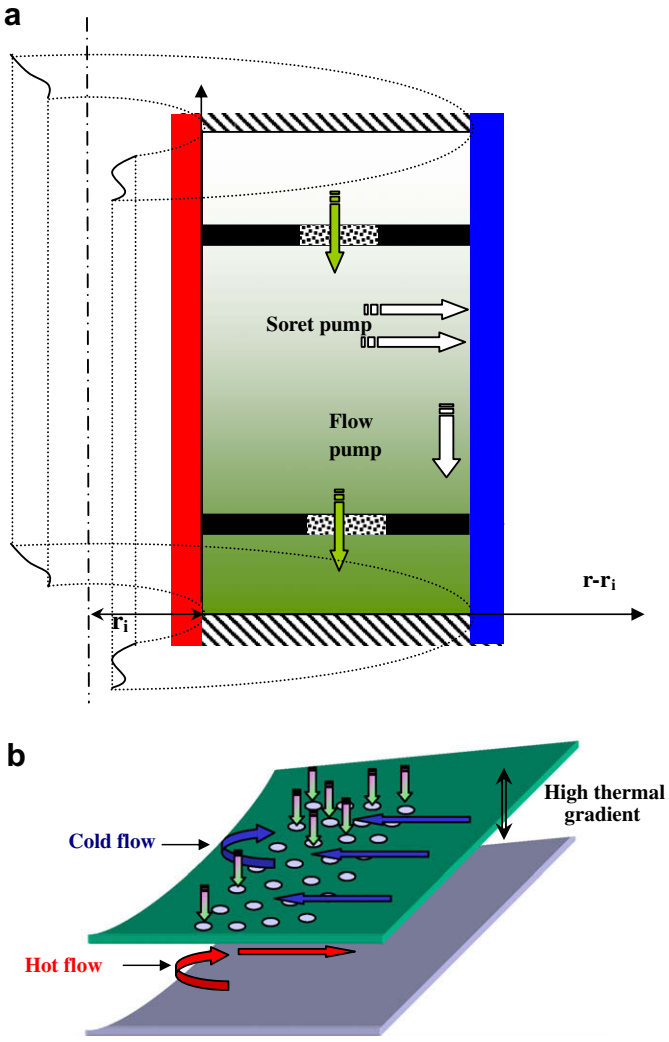

Fig. 7. Modified configuration with partitioning (a) and the included porous part for the specie transition (b).

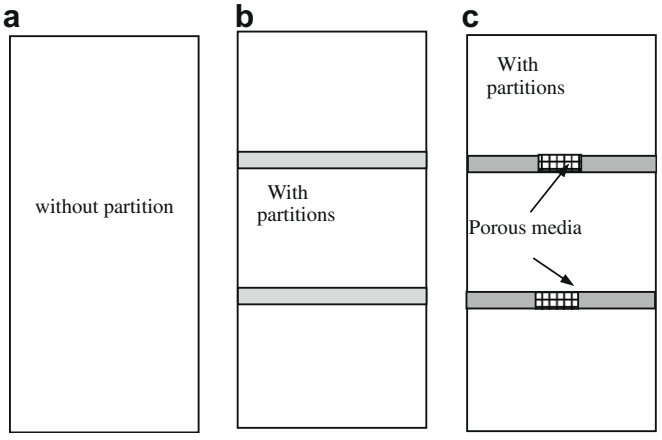

Fig. 8. The different considered cases, without partitions (a), with partition (b) and with partition including partial porous layer (c).

3. Partitioned domain in three part using solid horizontal walls with porous media in the central part. The porous size is from $x = 0.2$ to 0.3; the width is 0.03; $Da = 10^{-5}$, R = sol/liq = 0.1, $R_D = D_{por}/D_{liq} = 1$.

Fig. 9 shows the numerical results obtained for the corresponding non-partitioned domain (Fig. 9a), partitioned domain (Fig. 9b) and the partitioned with porous media through the horizontal (partitioning) plate (Fig. 9c).

The obtained flows in the three cases are clockwise rotating. The flow intensity is not strongly affected (b and c). The temperature field indicates that the flow is in fully boundary layer regime. The isotherms from Fig. 9b corroborate the strong vertical thermal gradient across the horizontal partitioning.

The solutal concentration difference obtained in the fully partitioned case is equivalent to the non-partitioning case. This is a direct consequence of non-communicating sub-domain. The initial concentration is C_0 and under equivalent horizontal temperature gradient (on each sub domain or fully domain) the obtained solutal field is almost the same. The weak effect is a consequence of flow

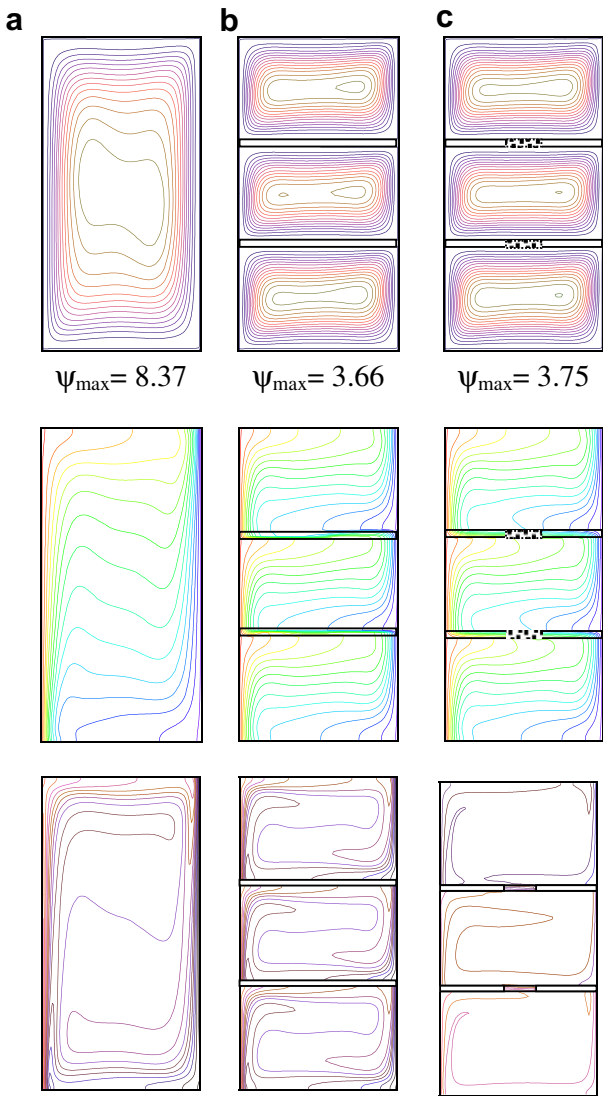

Fig. 9. Stream function, temperature and concentration; for full domain (a), partitioned domain (b) and partitioned-porous domain (c). ($Pr = 10$, $Le = 10$, $Ra_T = 5 \times 10^5$, $N = 0.0$, $r_{in} = 2$ and $A = 2$).

intensity decrease and the added local vertical temperature gradient in the vicinity of the partitioning plate.

In the third case and due to the porous layer the species pass from the upper sub-domain to the lower one due to the strong vertical temperature gradient. The temperature gradient and the temperature profile on the vertical mid-plan are represented in Fig. 10. The strong negative temperature gradient induces a strong thermodiffusion effect and a totally different concentration field is obtained. The steady state regime corresponds to no solutal transfer in the vertical direction. The corresponding solutal profile and the gradient along the vertical line are represented in Fig. 11. The higher species concentration is in the bottom of the cavity. Such high value is necessary in order to insure balance through the porous media, between the specie transfer under concentration gradient (Fick's law) and the specie transfer under thermodiffusion (temperature gradient) process.

The concentration profiles on the vertical mid plan obtained in the three analysed cases are represented in Fig. 11. This figure

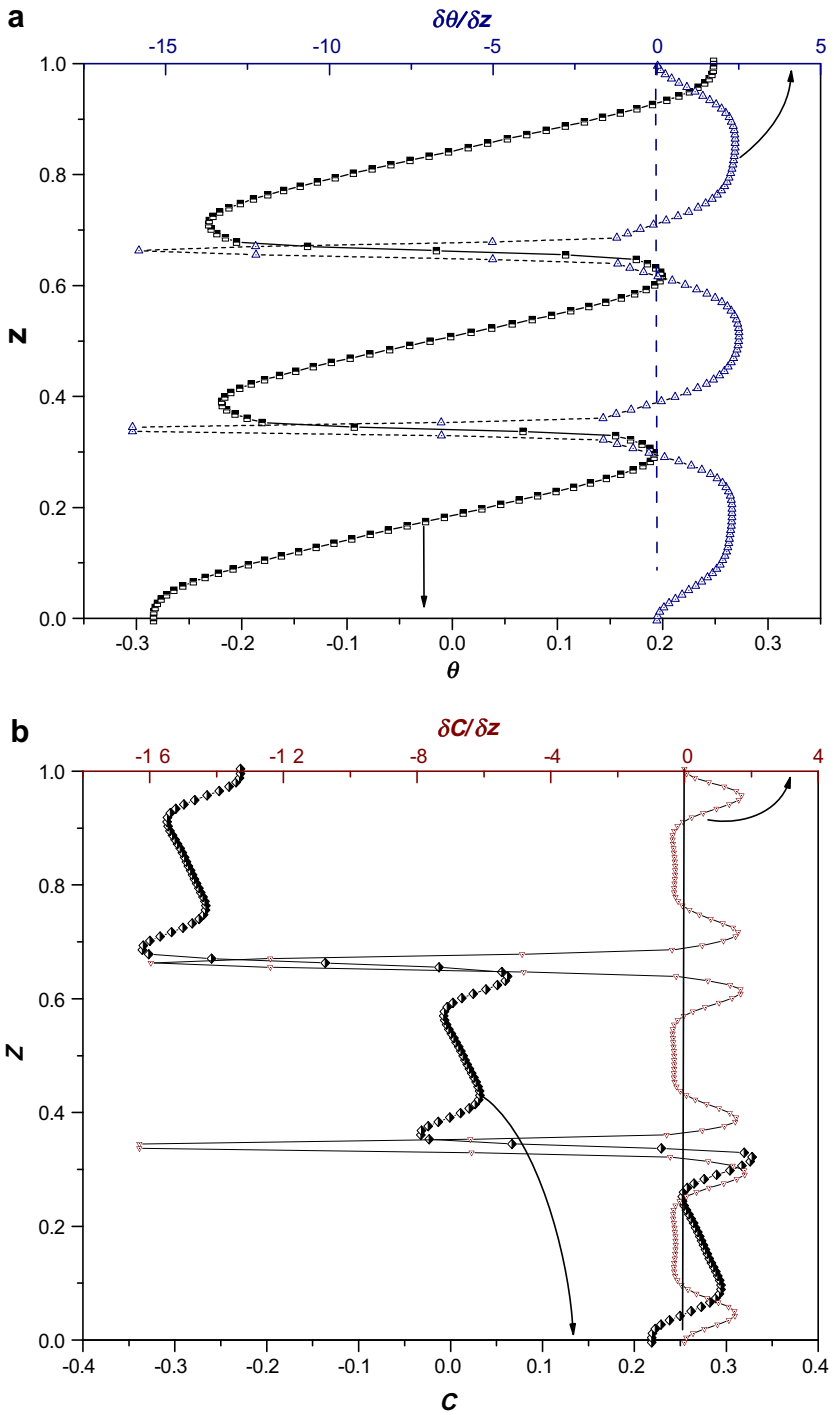

Fig. 10. Temperature profile and the corresponding gradient (a) and the concentration and the corresponding gradient (b) in the vertical mid-plan for the partitioned-porous domain, ($Pr = 10$, $Le = 10$, $Ra_T = 5 \times 10^5$, $N = 0.0$, $r_{in} = 2$ and $A = 2$).

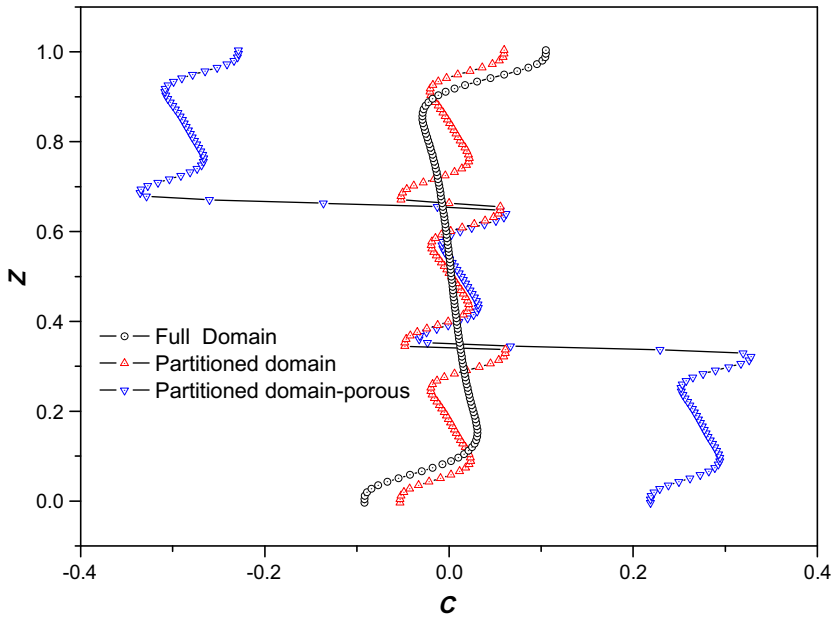

Fig. 11. Concentration profile in the vertical mid-plan for the full, partitioned and partitioned-porous domains ($Pr = 10$, $Le = 10$, $Ra_T = 5 \times 10^5$, $N = 0.0$, $r_{in} = 2$ and $A = 2$).

shows that concentration difference obtained in the full domain case and in the partitioned one is almost constant. It is also obvious the obtained increase in the concentration separation ability in the third case, *i.e.* partitioned-porous. Nevertheless the concentration difference tends to the asymptotic value obtained in diffusive situation but no more.

The observed improvement result from the temperature gradient across the partitioning and the increase in partitioning number will allow more separation ability. Three and four partitioning is compared with the same porous medium characteristics. The difference in the concentration profiles is shown in Fig. 12, where the separation increases with the partitioning number. The obtained maximum concentration difference over the full domain is summarised in Table 1. The obtained results demonstrate again the increase of the separation ability using porous partitioning. It also demonstrates that it is possible to overcome the classical identified asymptotic limit obtained in diffusive regime.

Nevertheless, we underline that the increase in partitioning number modifies the sub-domain height and the corresponding local Ra_T number. The resulting flow and the obtained fields are modified. The optimum global case will correspond to a multi-partitioning and where each sub-domain dimension corresponds to a Ra_T number equivalent to the optimum one (Fig. 5). The curvature coupling strategies will allow obtaining easily for a desired product.

4. Conclusion

The thermodiffusion, double-diffusive, natural convection within a vertical circular porous annulus was analysed. The Brinkman extended Darcy model is adapted.

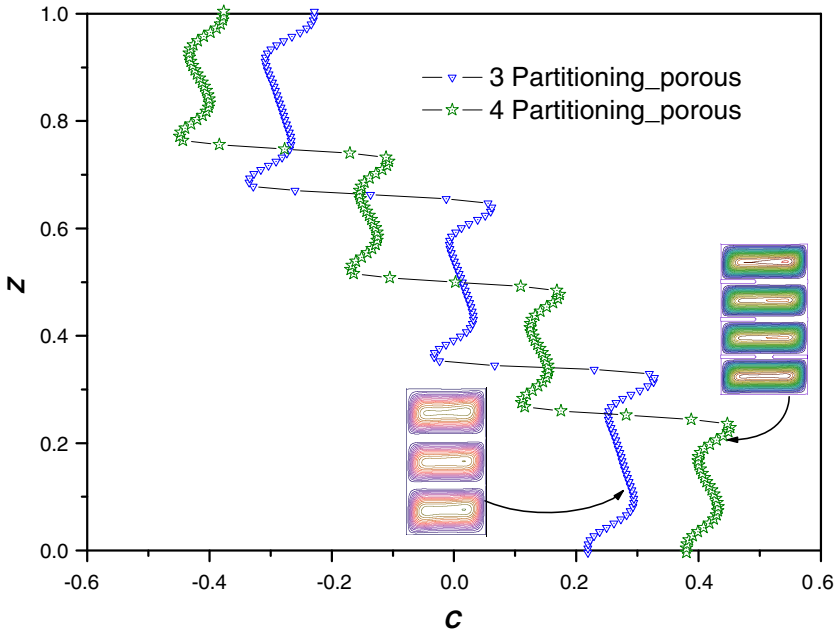

Fig. 12. Concentration profile in the vertical mid-plan for two partitioned- porous domains: 3 and 4 partitioning, ($Pr = 10$, $Le = 10$, $Ra_T = 5 \times 10^5$, $N = 0.0$, $r_{in} = 2$ and $A = 2$).

Table 1
The effect of chosen configuration on the maximum difference concentration.

	Diffusive	Convective Without porous connection			Convective With porous connection	
		One domain	3 domains	4 domains	3 domains	4 domains
Min C	−0.4789	−0.1871	−0.1767	−0.1587	−0.6810	−0.5782
Max C	0.5189	0.2089	0.1956	0.1748	0.4679	0.5942
ΔC	0.998 ($\sim$1)	0.3961	0.3724	0.3336	1.1488	1.1724

It was demonstrated that increase in the curvature of the cylindrical annulus permits a higher specie separation due to the non-symmetrical temperature profile.

The partitioning technique allows filtration separation. The separation ability increases with the partitioning number.

The new approach allows overcoming the classical admitted asymptotic ΔC limit corresponding to diffusive regime.

The present work illustrates the advantages of partition techniques with partial porous layers. It is suggested that a transient study is needed in order to demonstrate that the time needed to get such separation is lower that the classical one. The osmotic pressure in case of membrane technique is under study for transient case.

References

[1] K. Choukairy, R. Bennacer, M. El Ganaoui, Transient behaviours inside a vertical cylindrical enclosure heated from the sidewalls, Num. Heat Transfer Part A: Appl. 50 (8) (2006) 773–785.

[2] R. Bennacer, A.A. Mohamad, M. El Ganaoui, Analytical and numerical investigation of double diffusion in thermally anisotropy multilayer porous medium, Heat Mass Transfer 41 (2005) 298–305.

[3] R. Bennacer, M. El Ganaoui, P. Fauchais, On the thermal anisotropy affecting transfers in a multilayer porous medium, Comptes Rendus Mecanique 332 (7) (2004) 539–546.

[4] M.A. Havstad, P.J. Burns, Convective heat transfer in vertical cylindrical annuli filled. with a porous medium Int, J. Heat Mass Transfer 25 (1982) 1755–1765.

[5] D.C. Reda, Natural convection experiments in a liquid-saturated porous medium bounded by vertical coaxial cylinders, J. Heat Transfer 105 (1983) 795–802.

[6] V. Prasad, F.A. Kulacki, Natural convection in a vertical porous annulus, Int. J. Heat Mass Transfer 27 (1984) 207–219.

[7] V. Prasad, Numerical study of natural convection in a vertical, porous annulus with constant heat flux on the inner wall, Int. J. Heat Mass Transfer 29 (1986) 841–853.

[8] M. Hasnaoui, P. Vasseur, E. Bilgen, L. Robillard, Analytical and numerical study of natural convection heat transfer in a vertical porous annulus, Chem. Eng. Commun. 131 (1995) 141–159.

[9] H. Beji, R. Bennacer, R. Duval, P. Vasseur, Double diffusive natural convection in a vertical porous annulus, Num. Heat Part A 36 (1999) 153–170.

[10] R. Bennacer, H. Beji, R. Duval, P. Vasseur, The Brinkman model for thermosolutal convection in a vertical annular porous layer, Int. Commun. Heat Mass Transfer 27 (1) (2000) 69–80.

[11] J.K. Platten, J.C. Legros, Convection in liquids, Springer, Berlin, 1984 (Chapter 9).

[12] A. Mahidjiba, R. Bennacer, P. Vasseur, Effect of the boundary conditions on convection in a horizontal fluide layer with the soret contribution, Acta Mech. 160 (3–4) (2003) 161–177.

[13] J.P. Larre, J.K. Platten, G. Chavepeyer, Soret effect in ternary systems heated from below, Int. J. Heat Mass Transfer 40 (1997) 545–555.

[14] Ph. Traore, A. Mojtabi, Analyse de l'Effet Soret en Convection Thermosolutale, Entropie 184 (185) (1994) 32–37.

[15] G. Labrosse, Effet Soret et Convection naturelle 2D d'un liquide Binaire en Cavité Verticale Allongée, IV Colloque Interuniversitaire Franco-Québecois, Montréal, Canada, 1999, 333–338.

[16] R. Bennacer, A. Lakhal, H. Beji, M. Kessal, The Soret Effect on The Brinkman Model for Thermosolutal Convection in a Vertical Annular Porous Layer, in: A.A. Mohamad, R. Bennacer, Djerba-Tunisie (Eds.), Proceedings First International Conference on Applications of Porous Media, 2002, pp. 4–8.

[17] A. Lakhal, R. Bennacer, H. Beji, Effet de la thermodiffusion sur la convection en domaine annulaire: Solutions multiples, 16ème Congrès Français de Mécanique, Nice (2003) 1–5.

[18] S.V. Patankar, Num. Heat Transfer Fluid Flow, Hemisphere, New York, 1980.

[19] A. Mohamad, R. Bennacer, Natural convection in a confined saturated porous medium with horizontal temperature and vertical solutal gradients, Int. J. Therm. Sci. 40 (2001) 82–93.

[20] A. Tobbal, R. Bennacer, Heat and mass transfer in anisotropic porous layer reserch trend heat, Mass Momentum Transfer 3 (1998) 129–137.

[21] A. Lakhal, Separation Des Constituants En Utilisant L'effet Soret Dans Un Espace Annulaire, Ph.D. Thesis, Cergy Univ. France. 2004.